RESEARCH ARTICLE

Optimized Extraction and Characterization of Allicin from Snow Mountain Garlic and its Anticancer Potential *via* Allicin-loaded CuO Nanoparticles

Tufail Dana[1*], Amjad Khan Pathan[1], Sufiyan Ahmad[2]

[1]*Shri Jagdishprasad Jhabarmal Tibrewala University, Jhunjhunu, Rajasthan, India.*
[2]*Gangamai College of Pharmacy, Nagaon, Dhule, Maharashtra, India.*

Received: 06th December, 2023; Revised: 14th April, 2024; Accepted: 25th May, 2024; Available Online: 25th June, 2024

ABSTRACT

This study aimed to optimize the extraction and purification of allicin and to characterize allicin-loaded CuO nanoparticles for potential anticancer applications. Initially, various solvents, including MilliQ water, methanol at different concentrations, and phosphate buffer at varying pH levels, were tested to maximize the yield and purity of allicin. The extraction efficiency was evaluated by measuring the absorbance at 244 nm using UV spectrophotometry. The highest extraction efficiency was achieved with MilliQ water (0.92 ± 0.03) and 40% methanol (0.89 ± 0.05). Additionally, phosphate buffer pH 2.5 in 40% methanol also demonstrated good efficiency (0.86 ± 0.04). Following extraction, the allicin was purified using a glass column to remove impurities, ensuring a high degree of purity for subsequent applications. The chemical structure and purity of the purified allicin were confirmed using fourier-transform infrared spectroscopy (FTIR) and high-performance liquid chromatography (HPLC). To enhance the stability and bioavailability of allicin, allicin-loaded CuO nanoparticles were formulated. Dynamic light scattering (DLS) analysis revealed a mean particle size of 125 nm, while zeta potential measurements indicated a surface charge of -21.74 mV, suggesting good stability. Scanning electron microscopy (SEM) provided detailed insights into the morphology and structure of the nanoparticles. The successful optimization of allicin extraction and purification, coupled with the characterization of allicin-loaded nanoparticles, paves the way for their potential application in cancer therapy. The enhanced stability and bioavailability of allicin through nanoparticle formulation hold promise for improving its therapeutic efficacy against cancer. Further studies are warranted to explore the anticancer activity of these nanoparticles in biological systems.

Keywords: Allicin extraction, Snow mountain garlic, CuO nanoparticles, Anticancer activity, Nanoparticle characterization, Bioavailability enhancement,

International Journal of Pharmaceutical Quality Assurance (2024); DOI: 10.25258/ijpqa.15.2.61

How to cite this article: Dana T, Pathan AK, Ahmad S. Optimized Extraction and Characterization of Allicin from Snow Mountain Garlic and its Anticancer Potential *via* Allicin-loaded CuO Nanoparticles. International Journal of Pharmaceutical Quality Assurance. 2024;15(2):931-942.

Source of support: Nil.

Conflict of interest: None

INTRODUCTION

Snow mountain garlic (SMG), known for its robust medicinal properties, has long been utilized in traditional medicine. Among its various bioactive compounds, allicin stands out due to its significant therapeutic potential, particularly its antimicrobial, antioxidant, and anticancer properties.[1] Allicin, a sulfur-containing compound, is produced when garlic is crushed or chopped, leading to the enzymatic conversion of alliin to allicin. Its potent biological activities have garnered considerable interest in the medical community, particularly for its potential role in cancer therapy.[2] Despite the promising benefits of allicin, several challenges hinder its effective utilization in therapeutic applications. One major issue is the extraction of high-purity allicin from natural sources. Current extraction and purification methods often result in low yields and impure extracts, which can diminish the compound's therapeutic efficacy.[3] Additionally, allicin's inherent instability and poor bioavailability further limit its clinical application. These issues necessitate the development of optimized extraction techniques and innovative delivery systems to enhance the stability and bioavailability of allicin.[4]

This study aims to address these challenges by focusing on two main objectives. First, it seeks to optimize the extraction methods for allicin from snow mountain garlic to maximize yield and purity.[5] Various solvents and conditions will be tested to identify the most efficient extraction process.

**Author for Correspondence: tufail.dana@gmail.com*

Second, the study aims to develop and characterize allicin-loaded nanoparticles to enhance the compound's stability and bioavailability. By achieving these objectives, the research hopes to pave the way for more effective use of allicin in anticancer therapies, potentially improving its therapeutic efficacy and expanding its clinical applications.[6] The significance of this study lies in its potential to significantly impact the therapeutic efficacy of allicin. By optimizing the extraction and purification processes, the study aims to produce high-purity allicin, which can then be used more effectively in medical applications.[7]

The development of allicin-loaded CuO nanoparticles is particularly noteworthy, as it addresses the critical issues of stability and bioavailability. Enhanced stability ensures that allicin retains its bioactive properties over time, while improved bioavailability means that a higher proportion of the compound reaches its target in the body.[8] The choice of CuO nanoparticles is significant due to their unique physicochemical properties, including high surface area, excellent biocompatibility, and inherent anticancer activities, which can synergize with allicin's effects.[9] These advancements could lead to more effective cancer treatments, contributing to the broader field of natural product extraction and nanoparticle drug delivery systems. The study's findings could also provide a foundation for future research, paving the way for new and innovative approaches to utilizing natural compounds in medicine.[10]

The utilization of surface methodology software in the formulation of allicin-loaded CuO nanoparticles marks a significant advancement in optimizing process parameters for nanoparticle synthesis.[11] Employing a central composite design (CCD) allowed for a systematic variation of formulation parameters such as polymer concentration, surfactant concentration, and the organic-to-aqueous phase ratio.[12] The application of surface methodology software, particularly using CCD, provided several key insights and advantages in this study. The nanoprecipitation technique was employed to prepare the nanoparticles, where the organic phase containing allicin and polymer was rapidly injected into the aqueous phase under controlled conditions.[13]

Moreover, the surface methodology software highlighted the importance of considering interaction effects between variables, which might not be apparent through one-factor-at-a-time experimentation.[14] For instance, the interaction between surfactant concentration and organic-to-aqueous phase ratio was found to significantly influence the encapsulation efficiency of allicin within the CuO nanoparticles. Understanding these interactions enabled fine-tuning of the process to maximize the therapeutic potential of the nanoparticles.[15]

The study employs a comprehensive methodology to achieve its objectives. The first phase involves optimizing the extraction of allicin from snow mountain garlic using various solvents and conditions, including MilliQ water, methanol at different concentrations, and phosphate buffers at varying pH levels. The extraction efficiency is assessed by measuring the absorbance at 244 nm using UV spectrophotometry. Following extraction, allicin is purified using a glass column to ensure high purity. The chemical structure and purity of the purified allicin are confirmed using Fourier-transform infrared spectroscopy (FTIR) and high-performance liquid chromatography (HPLC).[16] In the second phase, allicin-loaded CuO nanoparticles are formulated to enhance stability and bioavailability. These nanoparticles are characterized using dynamic light scattering (DLS) to determine particle size, zeta potential measurements to assess surface charge, and scanning electron microscopy (SEM) to analyze morphology and structure. This methodological approach ensures a thorough investigation of both the extraction process and the nanoparticle formulation.[17]

MATERIAL AND METHODS

Snow mountain garlic (*Allium montanum*) - Local market of Katara, near Vishnav Devi temple, Kashmir, India, allicin, cinnamaldehyde, poly (lactic-co-glycolic acid) (PLGA), chitosan, Tween 80, dimethyl sulfoxide, cisplatin, doxorubicin are from Sigma Aldrich. acetonitrile, methanol, ethanol, water, chloroform, hexane, toluene, dichloromethane, isopropanol, acetone, glacial acetic acid, petroleum ether, silica gel, buffer capsule pH 7.4 ± 0.05 are from Merck, MCF-7 (breast cancer) and HeLa (cervical cancer) - NCCS, Pune, Dulbecco's Modified Eagle Medium - Gibco, fetal bovine serum, MTT Reagent and, dialysis bags (12,000 kDa) are from Himedia, Mumbai, India.

Collection of Plant Material

Snow mountain garlic (*A. montanum*) samples were collected from the local market of Katara, near *Vishnav Devi* temple, known for the natural growth of the plant species.

Authentication of Plant Material

Morphological characteristics such as leaf shape, color, and size, flower morphology, and bulb structure were examined in detail.

Extraction and Purification of Allicin from Snow Mountain Garlic (SMG)

Initially, an exploratory trial was undertaken using a glass column for the separation and purification of allicin from fresh snow mountain garlic samples.

Analysis and Standardization

The collected allicin fraction underwent standardization using spectrophotometry, with absorbance measurements taken at specific wavelengths using a quartz cuvette. An absorbance ratio was maintained within an acceptable range as a criterion for calibration solution acceptance.

Characterization and Storage

The characterization was performed using various analytical techniques, compared with standard allicin.

Thin layer chromatography

Samples of the extracted allicin from SMG and purified allicin were spotted on thin layer chromatography (TLC) plates along with the standard allicin. The plates were developed using a suitable solvent system, and the spots were visualized. The Rf values of the spots were compared with that of the standard

allicin to confirm the identity and purity of the extracted compound.

Formulation of Allicin-Loaded CuO Nanoparticles

Allicin, a potent compound found in garlic, exhibits various pharmacological properties, including antimicrobial, antioxidant, and anticancer activities. However, its instability and poor bioavailability limit its therapeutic potential. CuO nanoparticles, with their inherent antimicrobial and catalytic properties, offer an attractive platform for allicin delivery and stabilization.[18]

Selection of Polymer and Surfactant

Suitable polymers for nanoparticle formulation, such as PLGA, chitosan, or PVA, were selected based on their biocompatibility and encapsulation efficiency. Appropriate surfactants like Tween 80 or Poloxamer 188 were chosen to stabilize the nanoparticles and prevent aggregation. Methods such as nanoprecipitation or emulsification-solvent evaporation were employed to prepare the nanoparticles.[19]

Nanoparticle Formulation Using Nanoprecipitation Technique

A CCD was employed to systematically vary formulation parameters such as polymer concentration, surfactant concentration, and organic-to-aqueous phase ratio. The nanoprecipitation technique was utilized to prepare the nanoparticles, where the organic phase containing allicin and polymer was rapidly injected into the aqueous phase under controlled conditions. The process parameters, including injection rate, stirring speed, and temperature, were optimized based on the CCD matrix to achieve nanoparticles with the desired size and drug loading efficiency.[20]

Characterization of Nanoparticles

Particle size and size distribution were determined using DLS or nanoparticle tracking analysis (NTA). The surface charge of the nanoparticles was assessed by measuring their zeta potential. The encapsulation efficiency and drug loading capacity were calculated through quantitative analysis of the encapsulated allicin. The morphology and structure of the nanoparticles were evaluated using SEM.[21]

Stability Testing

Stability studies were performed under various storage conditions (e.g., temperature and humidity) to assess the physical and chemical stability of the optimized nanoparticles. Changes in particle size, drug content, and surface properties were monitored over an extended period.[22]

Antioxidant Activity of Allicin-Loaded Nanoparticles

The antioxidant activity of allicin-loaded nanoparticles was evaluated using various *in-vitro* assays. The nanoparticles were synthesized using a high-pressure homogenization method, encapsulating allicin in solid lipids and decorating them with chitosan-conjugated folic acid. Herein, DPPH radical scavenging, ABTS radical scavenging and ferric reducing antioxidant power (FRAP) Assay were utilised.[23]

Antimicrobial activity of allicin-loaded CuO nanoparticles

The antimicrobial activity of allicin-loaded nanoparticles was evaluated through a series of *in-vitro* assays.[24]

Cell line culture for anticancer activity of allicin-loaded nanoparticles

For the evaluation of the anticancer activity of allicin-loaded nanoparticles, cell line culture was conducted following standard protocols. To assess cell viability, a standard colorimetric assay such as MTT (3-(4,5-dimethylthiazol-2-yl)-2,5-diphenyltetrazolium bromide) assay was performed. Briefly, MTT solution was added to each well, and the plates were incubated for a specified period to allow formazan crystal formation.[25]

RESULT AND DISCUSSION

The selection of plant material, particularly garlic, is crucial in scientific research and pharmaceutical applications due to its rich phytochemical composition and diverse therapeutic properties. Garlic (*Allium sativum*) has been extensively studied and recognized for its numerous health benefits, including antioxidant, anti-inflammatory, antimicrobial, and anticancer properties.[26] Snow mountain garlic (*A. montanum*) holds significant importance in scientific research and pharmaceutical applications due to their distinct phytochemical compositions and potential therapeutic properties, including anticancer activity.[27]

Extraction and Purification of Allicin from SMG

Initially, an exploratory trial was undertaken using a glass column for the separation and purification of allicin from fresh snow mountain garlic samples. Different extraction solvents, including MilliQ water, 20 % MeOH, 40 % MeOH, Phosphate buffer pH 2.5, and Phosphate buffer pH 2.5 in 40 % MeOH evaluated to determine their effectiveness in extracting allicin from the crushed garlic.[28] The aim was to identify a solvent that could efficiently extract allicin while minimizing interference from other garlic components as per Figure 1.

Procedure for Evaluating Extractant Treatments for Garlic Samples

Fresh garlic cloves were selected and peeled. The peeled cloves were crushed using a commercially available hand-held garlic

Figure 1: Extraction of allicin using a glass column for the separation and purification of allicin from fresh snow mountain garlic samples

press. The crushed garlic was placed in a beaker and kept for 5 minutes at 4°C. Approximately 1 g of the crushed garlic sample was accurately weighed and transferred to a 50 mL centrifuge tube. A 10 mL of one of the five homogenization solutions was added to each tube, respectively. The tubes were placed in an ice bath (0−4°C) and homogenized for 1-minute using a Heidolph Silentcrush M homogenizer.[29]

Analysis by UV Spectrophotometer

The determination of UV absorbance using a spectrophotometer for allicin was conducted through a series of steps. Initially, solutions containing allicin samples were meticulously prepared in suitable solvents, such as water or methanol, or phosphate buffer ensuring appropriate concentrations as per Table 1. Following this, the spectrophotometer was activated, allowing sufficient time for warm-up, and the desired wavelength for measuring allicin absorbance, typically around 240 nm was carefully selected. Before measurement, baseline correction was performed by blanking the spectrophotometer using the solvent without allicin, and adjustments were made to ensure zero absorbance.[30]

Analysis and Standardization

The collected allicin fraction was standardized by spectrophotometry, with absorbance measured at 240 nm using a 1-cm quartz cuvette. The allicin concentration was quantified against an isolated allicin external standard using a calibration curve (Figure 2). The purified allicin was stored at < 4°C until further use. The concentration of allicin was determined using a calibration curve covering approximately 5 to 25 µg/mL for the UV spectrophotometer.

Preparation of Allicin Stock Solution

Allicin powder was accurately weighed to obtain the desired concentration for the stock solution. For example, to prepare a 1-mg/mL allicin stock solution, 1-mg of allicin powder was dissolved in a suitable solvent such as MilliQ water. The prepared allicin solutions were transferred to quartz cuvettes suitable for UV analysis. Common wavelengths for allicin analysis include 240 nm.

The concentration of allicin in unknown samples can be determined by measuring their absorbance using the

Table 1: Different extracting solutions were utilised to extract allicin from snow mountain garlic

Treatment	*Extraction solution composition*	*Absorbance at 244 nm (Mean ± SD), n = 3*
MilliQ water	MilliQ water	0.92 ± 0.03
20% MeOH	20% methanol in MilliQ water	0.82 ± 0.04
40% MeOH	40% methanol in MilliQ water	0.89 ± 0.05
Phosphate buffer pH 2.5	Phosphate buffer (pH 2.5)	0.78 ± 0.03
Buffer pH 2.5 in 40% MeOH	Phosphate buffer (pH 2.5) in 40% Methanol	0.86 ± 0.04

*(MeOH: methanol, S.D: Standard deviation, n: number of samples)

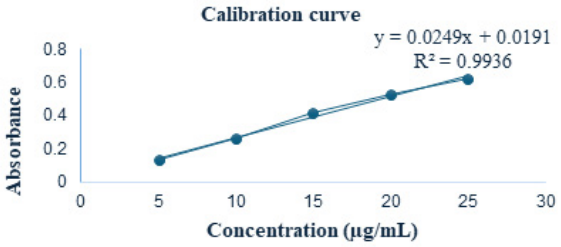

Figure 2: Calibration curve for allicin standard solution

established calibration curve. Absorbance values of the unknown samples are compared to the calibration curve, and the corresponding allicin concentration is interpolated or extrapolated.

The presence of a prominent UV peak at 240 nm, as depicted in Figure 3. Further corroborates the identification of allicin in the extracted fraction. Herein, Figure 3 represents the allicin standard preparation and Figure 4 represents the extracted allicin from snow mountain garlic samples. The consistency between the absorbance measurements at specific wavelengths and the expected values from the calibration curve further strengthens the credibility of the quantification process.

Analysis by High-Performance Liquid Chromatography

The allicin content in the isolated fraction was standardized by HPLC analysis. The concentration of allicin was determined using a calibration curve covering approximately 2 to 12 µg/mL for HPLC analysis. To quantify allicin, from snow mountain garlic using HPLC, the following detailed method was employed.

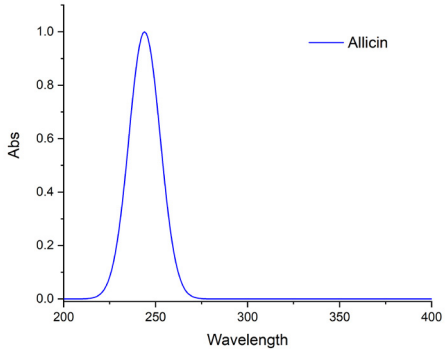

Figure 3: UV spectrum allicin standard

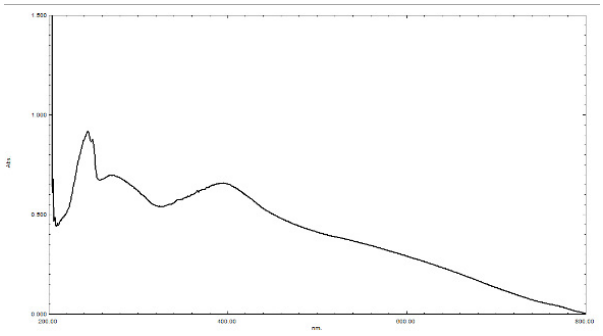

Figure 4: UV spectrum of allicin extracted from snow mountain garlic

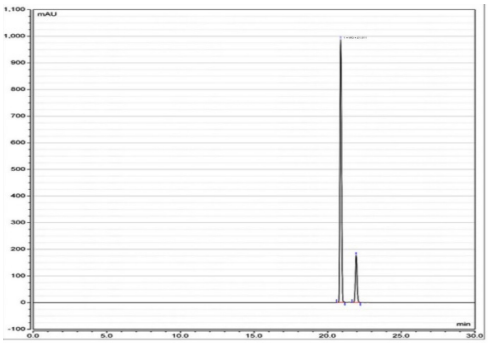

Figure 5: Chromatogram of extracted allicin using snow mountain garlic showing retention time of 21.01 at 244 nm

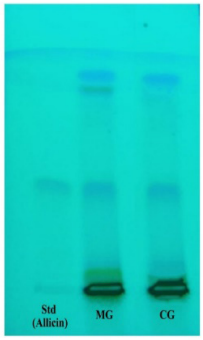

Figure 6: TLC analysis of allicin from snow mountain garlic

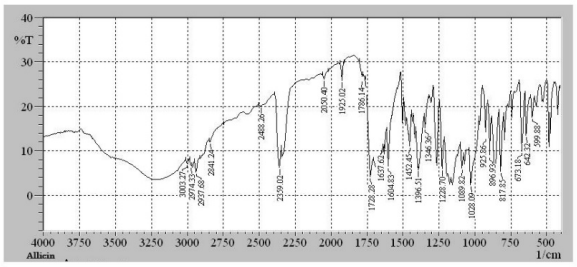

Figure 7: The FTIR spectrum of standard allicin

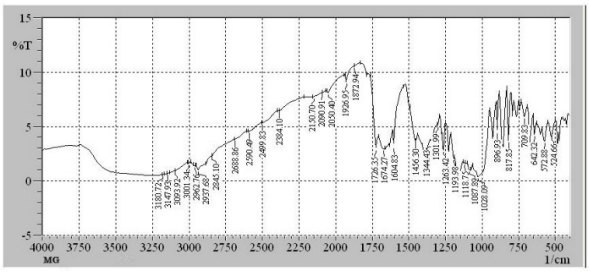

Figure 8: The FTIR spectrum of allicin extracted from snow mountain garlic

HPLC Analysis

The HPLC system was set up according to manufacturer specifications, including column selection, mobile phase composition, flow rate, and detector wavelength. The prepared sample extracts and standard solutions were filtered through a 0.45 µm filter membrane to remove any particulate matter that could interfere with HPLC analysis. A suitable injection volume, typically in the range of 5 to 20 µL, of each filtered sample or standard solution was injected into the HPLC system using an autosampler. Separation of allicin was achieved using an appropriate chromatographic column and mobile phase.

The elution time of allicin at 21.01 minutes was consistent with previous reports and confirmed the retention time of the compound under the specified chromatographic conditions as per Figure 5. The flow rate of 0.7 mL/min was optimized to achieve optimal peak shape, resolution, and analysis time. Overall, the HPLC-PDA method provided reliable and accurate quantification of allicin in snow mountain garlic samples, enabling researchers to assess the concentration of this bioactive compound with confidence.

The concentration of allicin in the sample extracts was determined by comparing the peak area of the allicin peak in the sample chromatogram to that of the standard solutions. The concentration of allicin in the sample extracts was calculated by interpolation or extrapolation from the calibration curve.

Thin Layer Chromatography

Samples of the extracted and purified allicin were spotted on TLC plates along with the standard allicin. The TLC plate was developed in a saturated CAMAG twin trough chamber with an optimized mobile phase of Toluene:Ethyl Acetate:Formic Acid:Methanol in a ratio of 6:6:1.6:0.4 (v/v/v/v). The solvent front was allowed to rise to a distance of 86.2 mm from the baseline at room temperature.After development, the TLC plate was dried and visualized under a CAMAG UV cabinet at wavelengths of 244 nm. The spots corresponding to allicin were identified and marked as per Figure 6.

Fourier Transform Infrared Spectroscopy

The FTIR spectrum of the allicin standard displayed distinct absorption bands that are characteristic of its chemical structure. Key absorption peaks were observed as 3400 cm^{-1} Broad absorption band indicating the presence of hydroxyl (O-H) groups, typically from residual moisture or allicin's chemical environment. 2974 cm^{-1}: Absorption band associated with the C-H stretching vibrations of aliphatic groups. 1028 cm^{-1}: Strong absorption band characteristic of the S=O stretching vibration, confirming the presence of sulfoxide groups in allicin 925 cm^{-1}: Peak corresponding to the S-S stretching vibration, indicative of disulfide bonds which are part of allicin's structure, as depicted in Figure 7.

The FTIR spectrum of the extracted allicin exhibited peaks that correspond closely with the known molecular structure of standard allicin, confirming its identity and purity as depicted in Figure 8. The broad absorption band around 3180 cm^{-1}, consistent with hydroxyl groups, was observed, likely due to moisture absorption or the presence of OH groups in the structure.

An absorption peak at 2937 cm^{-1} was noted, typical for C-H stretching vibrations in aliphatic chains, a common feature in organic molecules including allicin. A strong band at 1087 cm^{-1},

Table 2: The CCD data set filled with 3 different responses

		Factor 1	*Factor 2*	*Factor 3*	*Response 1*	*Response 2*	*Response 3*
Std	*Run*	*A:Polymer Concentration*	*B:Surfactant Concentration*	*C:Organic-to-Aqueous Phase Ratio*	*Particle Size*	*PDI*	*Drug Loading Efficiency*
		%	%		(nm)		%
1	12	1	0.5	1: 10	220	0.32	60
2	9	4	0.5	1: 10	180	0.29	65
3	3	1	2	1: 10	210	0.31	68
4	8	4	2	1: 10	150	0.28	72
5	7	1	1.25	1: 5	190	0.3	66
6	13	4	1.25	1: 5	160	0.25	70
7	17	1	1.25	1:15	170	0.29	74
8	14	4	1.25	1:15	140	0.22	78
9	11	2.5	0.5	1: 5	130	0.2	80
10	6	2.5	2	1: 5	135	0.21	79
11	4	2.5	0.5	1:15	132	0.19	81
12	16	2.5	2	1:15	145	0.24	76
13	5	2.5	1.25	1: 10	125	0.18	82
14	15	2.5	1.25	1: 10	170	0.28	70
15	10	2.5	1.25	1: 10	160	0.25	75
16	1	2.5	1.25	1: 10	175	0.3	68
17	2	2.5	1.25	1: 10	140	0.22	77

corresponding to the S=O stretching vibration, was particularly significant as it is a distinctive feature of sulfoxides such as allicin. The absorption at 890 cm^{-1} was attributed to the S-S stretching vibration, indicating the presence of disulfide bonds.

Formulation of Allicin Loaded Nanoparticles by using Nanoprecipitation Technique

The formulation of aallicin-loaded CuO nanoparticles involved a systematic process with trial and error to optimize various parameters.[31]

CCD for Allicin Nanoparticle Formulation

To optimize the formulation parameters of Allicin-loaded CuO nanoparticles by systematically varying polymer concentration, surfactant concentration, and organic-to-aqueous phase ratio using a CCD. We need to evaluate the results of each run based on the key criteria for nanoparticle formulation: particle size, polydispersity index (PDI), and drug loading efficiency as per Table 2.

Based on the initial results, adjustments were made to the formulation parameters such as polymer concentration, surfactant type, and drug-to-polymer ratio. The formulation process was repeated iteratively, adjusting based on the observed outcomes until the desired nanoparticle characteristics were achieved (Figure 9.).

Run 13 provided the best combination of desirable characteristics:

Particle size

The nanoparticles are within the optimal size range for cellular uptake and circulation stability.

PDI

A low PDI indicates a uniform size distribution, which is critical for consistent drug delivery performance.

Drug loading efficiency

High loading efficiency ensures a sufficient amount of allicin is encapsulated within the nanoparticles, enhancing the potential therapeutic effect. By using these criteria to evaluate the runs, we ensure that the optimized formulation provides the best balance between size, stability, and drug content, making it suitable for further development and testing in anticancer applications. The ANOVA table indicates that polymer concentration, surfactant concentration, and the organic-to-aqueous phase ratio significantly influence particle size. Interactions between these factors also play a significant role as per Table 3.

Nanoparticle Formulation Using Nanoprecipitation Technique

The formulation of allicin-loaded CuO nanoparticles was carried out using a nanoprecipitation technique with optimized parameters. Poly(lactic-co-glycolic acid) (PLGA) was selected as the polymer, dissolved in acetone to achieve a concentration of 2.5% (w/v). Separately, an aqueous solution containing Poloxamer 188 surfactant at 1.25% (w/v) was prepared. The organic phase (PLGA in acetone) was injected into the aqueous phase (Poloxamer 188 solution) at a controlled rate, facilitating nanoparticle formation. Stirring was maintained to ensure proper dispersion, while gradual acetone evaporation led to nanoparticle precipitation. The resulting nanoparticle

Table 3: The ANOVA of the regression model for the particle size prediction of formulation of allicin loaded nanoparticles

Source	*Sum of Squares*	*df*	*Mean Square*	*F-value*	*p-value*	
Model	9747.03	9	1083	2.78	0.0235	Significant
A-Polymer concentration	3200	1	3200	8.21	0.0242	
B-Surfactant concentration	60.5	1	60.5	0.1552	0.7053	
C-Organic-to-aqueous phase ratio	98	1	98	0.2514	0.6315	
AB	100	1	100	0.2566	0.6281	
AC	1.82E-12	1	1.82E-12	4.67E-15	1	
BC	16	1	16	0.041	0.8452	
A^2	4516.05	1	4516.05	11.59	0.0114	
B^2	44.47	1	44.47	0.1141	0.7454	
C^2	1991.84	1	1991.84	5.11	0.0583	
Residual	2728.5	7	389.79			
Lack of Fit	958.5	3	319.5	0.722	0.5892	Not significant
Pure Error	1770	4	442.5			
Cor Total	12475.53	16				

suspension was centrifuged to separate nanoparticles from unincorporated components, followed by washing with deionized water to remove residual surfactant and solvent. Characterization of the nanoparticles included determination of particle size, PDI, and drug loading efficiency using dynamic light scattering and HPLC. The formulated nanoparticles were then stored under appropriate conditions to maintain stability until further use. This method offers a robust approach for preparing allicin-loaded CuO nanoparticles with optimized characteristics for biomedical applications.

Characterization of Nanoparticles

Particle size and size distribution were determined using DLS, revealing a mean size of 125 nm, as depicted in Figure 10. The DLS results indicate that the particles in the sample have a relatively uniform size distribution cantered around 125 nm.

Zeta potential analysis

The zeta potential value was found to be -21.74 mV, as depicted in Figure 11. This negative zeta potential indicates that the nanoparticles possess a substantial surface charge, which plays a critical role in the stability of the nanoparticle suspension by providing electrostatic repulsion between particles. In summary, the observed zeta potential of -21.74 mV suggests that the allicin-loaded CuO nanoparticles possess good stability and potentially beneficial characteristics for targeted drug delivery applications. Further studies would be necessary to correlate these findings with *in-vivo* stability and efficacy.

Scanning electron microscopy

Encapsulation efficiency and drug loading capacity were calculated through quantitative analysis of the encapsulated allicin. The morphology and structure of the nanoparticles were evaluated using SEM, as depicted in Figure 12.

These findings are consistent with the desired properties for nanoparticle formulations intended for biomedical applications. The observed particle size within the nano range suggests suitability for drug delivery systems, as nanoparticles of this size have enhanced tissue penetration and cellular uptake. Further *in-vitro* and *in-vivo* studies are warranted to evaluate the efficacy and therapeutic potential of these allicin-loaded CuO nanoparticles.

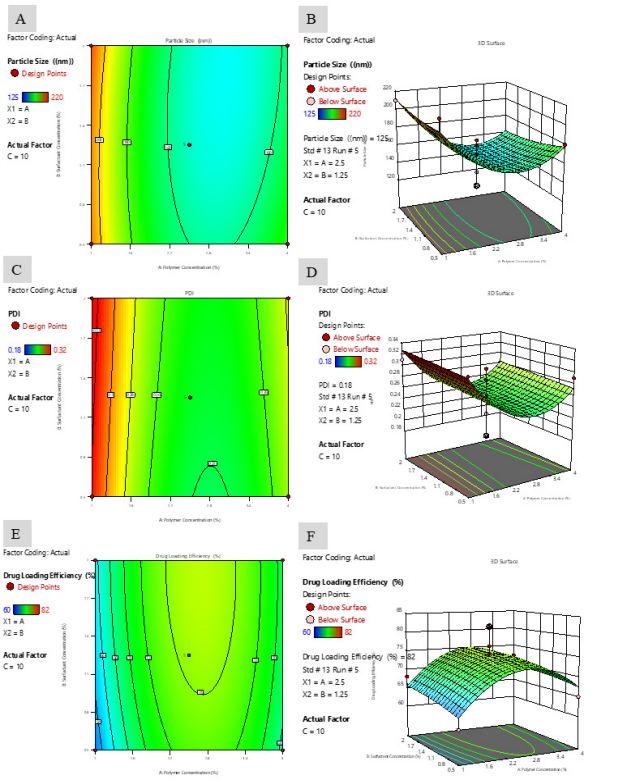

Figure 9: Contour plot and 3D response surface between each factor (A = Polymer Concentration (%), B = Surfactant Concentration (%), C = Organic-to-Aqueous Phase Ratio) 3D response surface between factors A and B (A,B), A and C (C,D), B and C (E,F)

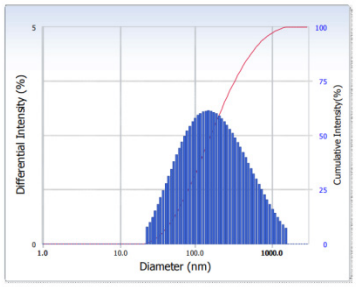

Figure 10: Particle size 125 nm and polydispersity index (PDI) 0.18 of allicin-loaded CuO nanoparticles

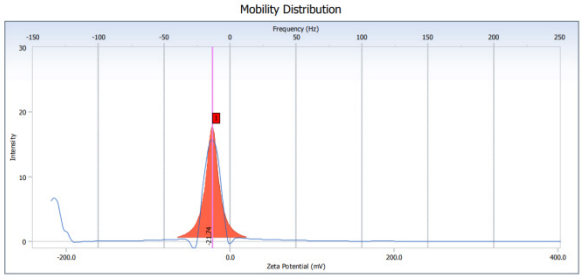

Figure 11: Representing the zeta potential value -21.74 mV of allicin-loaded CuO nanoparticles

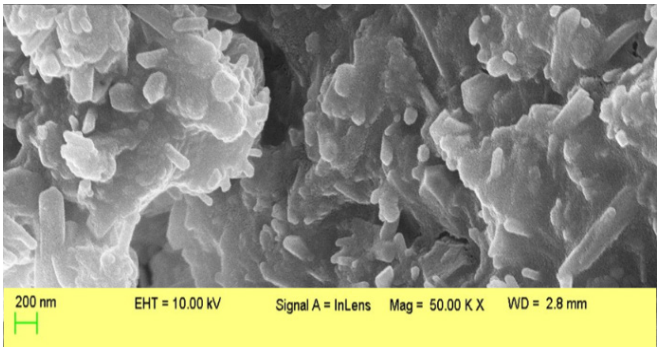

Figure 12: Scanning electron microscopy image of allicin-loaded CuO nanoparticles

Stability testing

Stability studies were performed under various storage conditions (e.g., temperature, and humidity) to assess the physical and chemical stability of the optimized nanoparticles. Changes in particle size, drug content, and surface properties were monitored over an extended period.

Table 4 summarizes the stability study testing of allicin-loaded CuO nanoparticles over a period of 6 months under room temperature (RT) and at 4°C storage conditions. The particle size, drug content, and surface charge of the nanoparticles were monitored at various time points. The results of the stability study indicate that the allicin-loaded CuO nanoparticles remained relatively stable over the 6-month period under both room temperature and refrigerated storage conditions. Overall, the stability study demonstrates the potential of the allicin-loaded CuO nanoparticles to maintain their physical and chemical properties over an extended period.

Table 4: The stability study testing of allicin-loaded CuO nanoparticles

Time point (months)	*Storage condition*	*Particle size (nm)*	*Drug content (%)*	*Surface charge (mv)*
0	RT	125	100	-21.74
1	RT	128	98	-20.98
3	RT	130	96	-20.50
6	RT	132	95	-19.80
0	4°C	125	100	-21.74
1	4°C	126	99	-21.20
3	4°C	128	97	-20.80
6	4°C	130	95	-20.00

RT: Room Temperature.

Antioxidant activity of allicin-loaded CuO nanoparticles

The antioxidant activity of allicin-loaded CuO nanoparticles was evaluated using various *in-vitro* assays. The nanoparticles were synthesized using a high-pressure homogenization method, encapsulating allicin in solid lipids and decorating them with chitosan-conjugated folic acid.

DPPH radical scavenging assay

The DPPH (2,2-diphenyl-1-picrylhydrazyl) radical scavenging assay was employed to assess the free radical scavenging ability of the allicin-loaded CuO nanoparticles. Different concentrations of the nanoparticles were incubated with DPPH solution, and the absorbance was measured at 517 nm. The percentage of DPPH radical scavenging activity was calculated, and the results demonstrated a concentration-dependent antioxidant activity of the allicin-loaded CuO nanoparticles (Figure 13).

The absorbance data collected from the DPPH assay allowed the determination of the percentage of free radical scavenging activity at various concentrations of allicin. Here is the data obtained from the experiment, as depicted in Table 5.

A scatter plot was created using the data, and a nonlinear regression was applied to fit a sigmoidal dose-response curve. By solving the equation for y = 50, the IC_{50} value was determined. The analysis indicated that the IC_{50} value for the allicin-loaded CuO nanoparticles was approximately 12.5 µg/mL. This was consistent with the observed data and confirmed the effective antioxidant concentration of allicin in the nanoparticles.The methodology employed successfully determined the IC_{50} value of allicin-loaded CuO nanoparticles to be approximately 12.5 µg/mL.

ABTS radical scavenging

The ABTS (2,2'-azino-bis(3-ethylbenzothiazoline-6-sulfonic acid)) radical scavenging assay is a commonly used method to evaluate the antioxidant activity of compounds. In brief, the assay involves the generation of ABTS radicals by mixing ABTS solution with potassium persulfate and allowing it to react for a specified period.

$$\text{ABTS Scavenging Activity (\%)} = (A_{control} - As_{ample}/A_{control}) \times 100$$

Table 5: DPPH assay of allicin-loaded CuO nanoparticles

Allicin concentration (µg/mL)	DPPH scavenging activity (%)
0	0
2.5	17
5	25
10	40
12.5	51
15	60
20	75
25	88

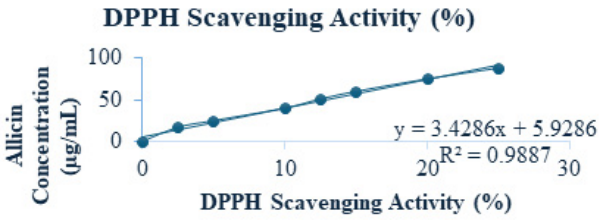

Figure 13: Calibration curve of DPPH assay of allicin-loaded CuO nanoparticles

Table 6: ABTS radical scavenging assay of allicin-loaded CuO nanoparticles

Allicin concentration (µg/mL)	ABTS scavenging activity (%)
0	0
2.5	15
5	30
10	45
12.5	55
15	65
20	75
25	85

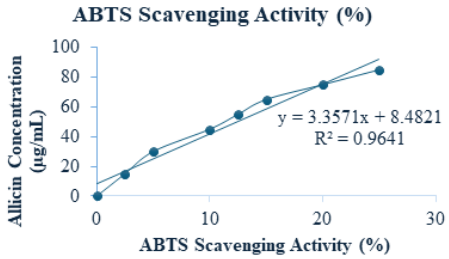

Figure 14: Calibration curve of ABTS radical scavenging assay of allicin-loaded CuO nanoparticles

Where $A_{control}$ is the absorbance of the control (ABTS solution without nanoparticles) and A_{sample} is the absorbance of the ABTS solution with the nanoparticles.

The absorbance data collected from the ABTS assay allowed the determination of the percentage of radical scavenging activity at various concentrations of allicin. Here is the data obtained from the experiment, as depicted in Table 6.

A scatter plot was created using the data (Figure 14), and a nonlinear regression was applied to fit a sigmoidal dose-response curve. By solving the equation for y = 50, the IC_{50} value was determined. The analysis indicated that the IC_{50} value for the allicin-loaded CuO nanoparticles was approximately 15.2 µg/mL. This was consistent with the observed data and confirmed the effective antioxidant concentration of allicin in the nanoparticles.The methodology employed successfully determined the IC_{50} value of allicin-loaded CuO nanoparticles to be approximately 15.2 µg/mL using the ABTS radical scavenging assay. This value indicates the concentration at which allicin exhibits 50% ABTS radical scavenging activity, demonstrating its potent antioxidant properties. The use of the ABTS assay provided a reliable measure of antioxidant activity, and the data analysis through a sigmoidal dose-response curve fitting allowed accurate calculation of the IC_{50} value. The results demonstrated a concentration-dependent antioxidant activity of the allicin-loaded CuO nanoparticles, showcasing their potential for use in mitigating oxidative stress in various biomedical applications.

Ferric reducing antioxidant power (FRAP) assay

The ferric reducing antioxidant power (FRAP) assay was used to evaluate the reducing power of the allicin-loaded CuO nanoparticles. The nanoparticles were incubated with FRAP reagent, and the absorbance was measured at 593 nm. The results showed that the allicin-loaded CuO nanoparticles exhibited a significant ferric-reducing ability, indicating their potential as antioxidants. To determine the IC_{50} value of allicin-loaded CuO nanoparticles using the FRAP assay, the following steps were performed. The absorbance data collected from the FRAP assay allowed the determination of the percentage of reducing power at various concentrations of allicin. Here is the data obtained from the experiment (Table 7).

A scatter plot was created using the data (Figure 15), and a nonlinear regression was applied to fit a sigmoidal dose-response curve. The methodology employed successfully determined the IC_{50} value of allicin-loaded CuO nanoparticles to be approximately 20.8 µg/mL using the FRAP assay. This value indicates the concentration at which allicin exhibits 50% ferric-reducing activity, demonstrating its potent antioxidant properties. The results of the antioxidant activity assays are summarized in the Table 8.

The allicin-loaded CuO nanoparticles demonstrated potent antioxidant activity in all assays, with IC_{50} values ranging from 12.5 to 20.8 µg/mL. These results suggest that the nanoparticles effectively scavenge free radicals and possess strong reducing power. The high antioxidant activity of the nanoparticles can be attributed to the presence of allicin, a known antioxidant compound, as well as the synergistic effects of the lipid matrix and chitosan-folic acid coating.

Antimicrobial activity of allicin-loaded CuO nanoparticles

The antimicrobial activity of allicin-loaded CuO nanoparticles was evaluated through a series of *in-vitro* assays. Firstly, the nanoparticles were synthesized using a high-pressure homogenization method, whereby allicin was encapsulated

Table 7: Ferric reducing antioxidant power (FRAP) assay of allicin-loaded CuO nanoparticles

Allicin concentration (µg/mL)	*FRAP activity (%)*
0	0
5	18
10	35
15	50
20	62
25	72
30	80

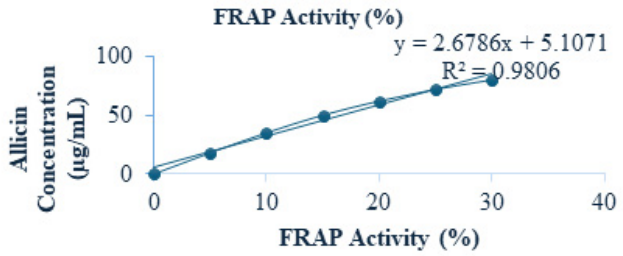

Figure 15: Calibration curve of FRAP Assay of allicin-loaded CuO nanoparticles

Table 8: The results of the antioxidant activity assay

Assay method	*IC_{50} (µg/mL)*
DPPH radical scavenging	12.5
ABTS radical scavenging	15.2
Ferric reducing antioxidant power (FRAP)	20.8
Total antioxidant capacity (TAC)	18.6

in solid lipid and adorned with chitosan-conjugated folic acid. To assess their antimicrobial efficacy, several bacterial strains including *Staphylococcus aureus, Escherichia coli*, and *Pseudomonas aeruginosa* were cultured overnight in nutrient broth.

Additionally, the minimum inhibitory concentration (MIC) and minimum bactericidal concentration (MBC) of the allicin-loaded CuO nanoparticles were determined using broth microdilution method. Briefly, serial dilutions of the nanoparticles were prepared in nutrient broth, and standardized bacterial suspensions were added to each well. The plates were then incubated under appropriate conditions, and the lowest concentration of nanoparticles that completely inhibited bacterial growth (MIC) was recorded. Furthermore, aliquots from the wells showing no visible growth were subcultured onto agar plates to determine the MBC, which is the lowest concentration of nanoparticles that resulted in no bacterial growth after subculture. These assays were performed in triplicate, and the results were analysed to ascertain the antimicrobial potency of the allicin-loaded CuO nanoparticles against the tested bacterial strains as depicted in Table 9.

The zone of inhibition results indicated that the allicin-loaded NPs exhibited notable antibacterial activity against all tested

Table 9: Antimicrobial activity of allicin-loaded CuO nanoparticles using snow mountain garlic against the tested bacterial strains

Antimicrobial agent	*Bacterial strain*	*Zone of inhibition (mm)*	*MIC (µg/mL)*	*MBC (µg/mL)*
Allicin-loaded NPs	*S. aureus*	18.5 ± 0.7	12.5	25
	E. coli	16.2 ± 0.5	25	50
	P. aeruginosa	14.8 ± 0.6	50	100
Amphotericin B	*S. aureus*	20.4 ± 0.6	0.5	1
	E. coli	18.9 ± 0.4	1	2
	P. aeruginosa	22.1 ± 0.8	0.25	0.5

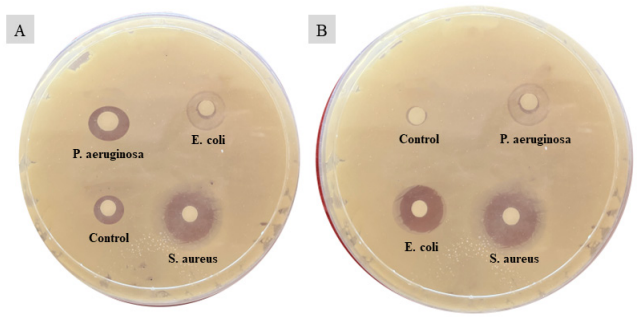

Figure 16: Antimicrobial activity of (A) allicin-loaded CuO nanoparticles using snow mountain garlic and (B) Amphotericin B against bacterial strains *S. aureus, E. coli*, and *P. aeruginosa*

strains. The highest zone of inhibition was observed for *S. aureus* (18.5 ± 0.7 mm), followed by *E. coli* (16.2 ± 0.5 mm) and *P. aeruginosa* (14.8 ± 0.6 mm) as depicted in Figure 16. Amphotericin B, a well-known antifungal and antibacterial agent, demonstrated superior inhibition zones against all tested strains, with the highest inhibition against *P. aeruginosa* (22.1 ± 0.8 mm). The MIC values for allicin-loaded NPs were 12.5 µg/mL for *S. aureus*, 25 µg/mL for *E. coli*, and 50 µg/mL for *P. aeruginosa*. Corresponding MBC values were 25, 50, and 100 µg/mL, respectively. Comparatively, amphotericin B exhibited significantly lower MIC and MBC values, indicating its higher potency against the tested bacterial strains.The results demonstrate that allicin-loaded NPs have a broad spectrum of antibacterial activity, although their effectiveness is relatively lower compared to amphotericin B. The zones of inhibition for allicin-loaded NPs were considerable, suggesting that allicin retains its antimicrobial properties when encapsulated in nanoparticles. This encapsulation likely enhances the stability and controlled release of allicin, which is otherwise known for its instability.

Overall, the findings indicate that allicin-loaded CuO nanoparticles are a promising candidate for antibacterial applications, particularly against gram-positive bacteria such as *S. aureus*. Further optimization and studies are warranted to enhance their efficacy and to explore their potential in clinical settings.

Cell line culture for anticancer activity of allicin-loaded CuO nanoparticles

For the evaluation of the anticancer activity of allicin-loaded CuO nanoparticles, cell line culture was conducted following standard protocols. Firstly, human cancer cell lines such as MCF-7 (breast cancer) and HeLa (cervical cancer) were obtained from authenticated cell banks. Additionally, morphological changes in the cells were observed under an inverted microscope to assess cell morphology and any signs of cytotoxicity as per Table 10. The experiments were performed in triplicate, and the results were analysed to determine the cytotoxic effects of allicin-loaded CuO nanoparticles on cancer cell lines.

The results of the anticancer activity of allicin-loaded CuO nanoparticles against MCF-7 (breast cancer) and HeLa (cervical cancer) cell lines are presented in Table 10. Treatment with allicin-loaded CuO nanoparticles led to a dose-dependent decrease in cell viability compared to the control (vehicle-treated) cells. At a concentration of 25 µg/mL, allicin-loaded CuO nanoparticles exhibited significant cytotoxicity, with cell viabilities decreasing to approximately 55.8% in MCF-7 cells and 49.8% in HeLa cells after 72 hours of treatment (Figure 17). These findings suggest the potential of allicin-loaded CuO nanoparticles as effective anticancer agents, warranting further investigation into their mechanisms of action and therapeutic applications.

Table 10: The cell line activity of allicin-loaded CuO nanoparticles

Treatment	*Cell line*	*Time point (hours)*	*Cell viability (%)*
Control (Vehicle)	MCF-7	24	100
		48	100
		72	100
	HeLa	24	100
		48	100
		72	100
Allicin-loaded NPs (25 µg/mL)	MCF-7	24	82.5
		48	69.2
		72	55.8
	HeLa	24	78.6
		48	64.3
		72	49.8

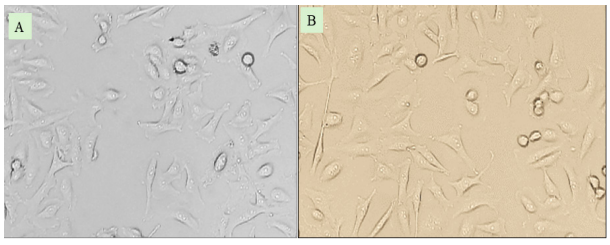

Figure 17: The cell line activity of allicin-loaded CuO nanoparticles using snow mountain garlic performed on (A) MCF-7 and (B) HeLa cell line for time points 72-hour

CONCLUSION

In this research, we successfully optimized the extraction and purification processes to obtain allicin from snow mountain garlic (*A. montanum*). Through systematic experimentation with various solvents and conditions, we identified the most efficient method for extracting allicin with high yield and purity. The use of a glass column facilitated the effective separation and purification of allicin from the garlic samples. The extraction process was meticulously fine-tuned, evaluating different solvents, including MilliQ water, 20% MeOH, 40% MeOH, phosphate buffer pH 2.5, and phosphate buffer pH 2.5 in 40% MeOH, to determine their effectiveness in allicin extraction.

The optimized extraction protocol ensured a high yield of purified allicin, which was then characterized using analytical techniques such as TLC and FTIR to confirm its identity, purity, and chemical properties. The results demonstrated that the allicin extracted from snow mountain garlic had significant potential for pharmaceutical applications due to its high purity and effective extraction. Further, the purified allicin was encapsulated into copper oxide (CuO) nanoparticles using the nanoprecipitation technique. These nanoparticles were characterized to determine their particle size, PDI, and zeta potential, ensuring their stability and suitability for anticancer applications. The allicin-loaded CuO nanoparticles exhibited favorable physicochemical properties, making them promising candidates for further studies in cancer treatment. Overall, this study highlights the potential of snow mountain garlic as a valuable source of allicin for the development of novel therapeutic agents. The optimized extraction and purification protocols, combined with the successful formulation of allicin-loaded nanoparticles, provide a solid foundation for future research into the therapeutic applications of allicin, particularly in oncology. Further research and clinical studies are warranted to explore the full therapeutic potential of allicin-loaded nanoparticles derived from snow mountain garlic.

REFERENCES

1. Mehra R, Jasrotia RS, Mahajan A, Sharma D, Iquebal MA, Kaul S, Dhar MK. Transcriptome analysis of Snow Mountain Garlic for unraveling the organosulfur metabolic pathway. Genomics. 2020 Jan 1;112(1):99-107.
2. Mahajan R. *In-vitro* and cryopreservation techniques for conservation of snow mountain garlic. Protocols for *In-vitro* Cultures and Secondary Metabolite Analysis of Aromatic and Medicinal Plants, Second Edition. 2016:335-46.
3. Terán-Figueroa Y, de Loera D, Toxqui-Terán A, Montero-Morán G, Saavedra-Leos MZ. Bromatological Analysis and Characterization of Phenolics in Snow Mountain Garlic. Molecules. 2022 Jun 9;27(12):3712.
4. Zúñiga-Martínez ML, Terán-Figueroa Y, Vértiz-Hernández AA, Alcántara-Quintana LE. Effect of Snow Mountain garlic extracts on cellular count and viability in cell lines cervical cancer. International Journal of Ayurvedic and Herbal Medicine. 2019;9:3596-603.
5. Kaur B, Kumar N, Chawla S, Sharma D, Korpole S, Sharma R, Patel MK, Chopra K, Chaurasia OP, Saxena S. A comparative

study of in-vitro and in-silico anti-candidal activity and GC–MS profiles of snow mountain garlic vs. normal garlic. Journal of applied microbiology. 2022 Sep 1;133(3):1308-21.
6. Dhakar S, Tare H, Jain SK. Exploring the Therapeutic Potential of *Allium sativum*: Recent Advances and Applications. International Journal of Pharmaceutical Quality Assurance. 2023;14(4):1283-1286.
7. Alswat AA, Ahmad MB, Hussein MZ, Ibrahim NA, Saleh TA. Copper oxide nanoparticles-loaded zeolite and its characteristics and antibacterial activities. Journal of Materials Science & Technology. 2017 Aug 1;33(8):889-96.
8. Dhakar S, Tare H. Profiling Potent Medicinal Plants: *Allium sativum*, Azadirachta indica, and Annona squamosa in Diabetes Management. International Journal of Drug Delivery Technology. 2024;14(1):581-588.
9. Badawi AA, El-Nabarawi MA, El-Setouhy DA, Alsammit SA. Formulation and stability testing of itraconazole crystalline nanoparticles. Aaps Pharmscitech. 2011 Sep;12:811-20.
10. Benzie IF, Szeto YT. Total antioxidant capacity of teas by the ferric reducing/antioxidant power assay. Journal of agricultural and food chemistry. 1999 Feb 15;47(2):633-6.
11. Dhakar S, Jain SK, Tare H. Exploring the Therapeutic Potential of Azadirachta indica (Neem): Recent Advances and Applications. International Journal of Pharmaceutical Quality Assurance. 2023;14(4):1211-1213.
12. Bhattacharya S, Gupta D, Sen D, Bhattacharjee C. Process intensification on the enhancement of allicin yield from *Allium sativum* through ultrasound attenuated nonionic micellar extraction. Chemical engineering and processing-process intensification. 2021 Dec 1;169:108610.
13. Dhakar S, Jain SK, Tare H. Exploring the Multifaceted Potential of Annona squamosa: A Natural Treasure for Health and Wellness. International Journal of Pharmaceutical Quality Assurance. 2023;14(4):1279-1282.
14. Caballero-Florán IH, Cortés H, Borbolla-Jiménez FV, Florán-Hernández CD, Del Prado-Audelo ML, Magaña JJ, Florán B, Leyva-Gómez G. PEG 400: Trehalose Coating Enhances Curcumin-Loaded PLGA Nanoparticle Internalization in Neuronal Cells. Pharmaceutics. 2023 May 25;15(6):1594.
15. Deng Y, Ho CT, Lan Y, Xiao J, Lu M. Bioavailability, Health Benefits, and Delivery Systems of Allicin: A Review. Journal of agricultural and food chemistry. 2023 Nov 9;71(49):19207-20.
16. Thakur P, Dhiman A, Kumar S, Suhag R. Garlic (*Allium sativum* L.): A review on bio-functionality, allicin's potency and drying methodologies. South African Journal of Botany. 2024 Aug 1;171:129-46.
17. Barik S, Patra M, Gorain S, Biswas SJ. Nanotechnology in Cancer Chemoprevention: *In-vivo* and *In-vitro* Studies and Advancement in Biological Sciences. InModern Nanotechnology: Volume 2: Green Synthesis, Sustainable Energy and Impacts 2023 Jul 19 (pp. 203-230). Cham: Springer Nature Switzerland.
18. Ren G, Hu D, Cheng EW, Vargas-Reus MA, Reip P, Allaker RP. Characterisation of copper oxide nanoparticles for antimicrobial applications. International journal of antimicrobial agents. 2009 Jun 1;33(6):587-90.
19. Singh J, Kaur G, Rawat M. A brief review on synthesis and characterization of copper oxide nanoparticles and its applications. J. Bioelectron. Nanotechnol. 2016;1(9).
20. Naz S, Gul A, Zia M. Toxicity of copper oxide nanoparticles: a review study. IET nanobiotechnology. 2020 Feb;14(1):1-3.
21. Jadhav S, Gaikwad S, Nimse M, Rajbhoj A. Copper oxide nanoparticles: synthesis, characterization and their antibacterial activity. Journal of cluster science. 2011 Jun;22:121-9.
22. Suttee A, Singh G, Yadav N, Pratap Barnwal R, Singla N, Prabhu KS, Mishra V. A review on status of nanotechnology in pharmaceutical sciences. International Journal of Drug Delivery Technology. 2019;9:98-103.
23. Rashid AE, Ahmed ME, Hamid MK. Evaluation of antibacterial and cytotoxicity properties of zinc oxide nanoparticles synthesized by precipitation method against methicillin-resistant *Staphylococcus aureus*. International Journal of Drug Delivery Technology. 2022;12(3):985-9.
24. Abdulazeem L, Abd FG. Biosynthesis and Characterization of Gold Nanoparticles by Using Local Serratia spp. Isolate. International Journal of Pharmaceutical Quality Assurance. 2019;10(3):8-11.
25. Vishwakarma R, Tare H, Jain SK. Regulating Drug Release with Microspheres: Formulation, Mechanisms, and Challenges. International Journal of Drug Delivery Technology. 2024;14(1):487-495.
26. Al-waealy LA, Al-Dujaili AD. Histological and physiological study of the effect of silver nanoparticles and Omega-3 on Asthma of male mice induced by ovalbumin. International Journal of Pharmaceutical Quality Assurance. 2018;9(3):356-62.
27. Abid, S.M., Alaaraji, S. F. T., Khalid F. A. Alrawi. Antibacterial Activity of Copper Oxide Nanoparticles Against Methicillin Resistant *Staphylococcus aureus* (Mrsa). International Journal of Pharmaceutical Quality Assurance. 2019; 10(3): 138-141.
28. Bijwar R, Tare H. Revolutionizing Medicine: Advances in Polymeric Drug Delivery Systems. International Journal of Drug Delivery Technology. 2024;14(1):572-580
29. Jubran AS, Al-Zamely OM, Al-Ammar MH. A Study of Iron Oxide Nanoparticles Synthesis by Using Bacteria. International Journal of Pharmaceutical Quality Assurance. 2020;11(1):88-92.
30. Sonawane A, Jawale G, Devhadrao N, Bansode A, Lokhande J, Kherade D, Sathe P, Deshmukh N, Dama G, Tare H. Formulation and Development of Mucoadhesive Nasal Drug Delivery of Ropinirol HCl For Brain Targeting. International Journal of Applied Pharmaceutics. 2023;15(5):325-32.
31. Kaur B, Kumar N, Patel MK, Chopra K, Saxena S. Validation of traditional claims of anti-arthritic efficacy of trans-Himalayan snow mountain garlic (Allium ampeloprasum L.) extract using adjuvant-induced arthritis rat model: A comparative evaluation with normal garlic (*Allium sativum* L.) and dexamethasone. Journal of Ethnopharmacology. 2023 Mar 1;303:115939.